Am J Physiol Lung Cell Mol Physiol 311: L985–L999, 2016.
First published September 30, 2016; doi:10.1152/ajplung.00345.2016.

Simvastatin prevents and reverses chronic pulmonary hypertension in newborn rats via pleiotropic inhibition of RhoA signaling

Mathew J. Wong,[1,4] Crystal Kantores,[1] Julijana Ivanovska,[1] Amish Jain,[2,3,4] and Robert P. Jankov[1,2,3,4]

[1]*Physiology & Experimental Medicine Program, Hospital for Sick Children Research Institute, Toronto, Ontario, Canada;* [2]*Heart and Stroke Richard Lewar Centre of Excellence in Cardiovascular Research, University of Toronto, Toronto, Ontario, Canada;* [3]*Department of Paediatrics, Faculty of Medicine, University of Toronto, Toronto, Ontario, Canada; and* [4]*Department of Physiology, Faculty of Medicine, University of Toronto, Toronto, Ontario, Canada*

Submitted 9 August 2016; accepted in final form 30 September 2016

Wong MJ, Kantores C, Ivanovska J, Jain A, Jankov RP. Simvastatin prevents and reverses chronic pulmonary hypertension in newborn rats via pleiotropic inhibition of RhoA signaling. *Am J Physiol Lung Cell Mol Physiol* 311: L985–L999, 2016. First published September 30, 2016; doi:10.1152/ajplung.00345.2016.—Chronic neonatal pulmonary hypertension (PHT) frequently results in early death. Systemically administered Rho-kinase (ROCK) inhibitors prevent and reverse chronic PHT in neonatal rats, but at the cost of severe adverse effects, including systemic hypotension and growth restriction. Simvastatin has pleiotropic inhibitory effects on isoprenoid intermediates that may limit activity of RhoA, which signals upstream of ROCK. We therefore hypothesized that statin treatment would safely limit pulmonary vascular RhoA activity and prevent and reverse experimental chronic neonatal PHT via downstream inhibitory effects on pathological ROCK activity. Sprague-Dawley rats in normoxia (room air) or moderate normobaric hypoxia (13% O_2) received simvastatin (2 $mg \cdot kg^{-1} \cdot day^{-1}$ ip) or vehicle from postnatal days 1–14 (prevention protocol) or from days 14–21 (rescue protocol). Chronic hypoxia increased RhoA and ROCK activity in lung tissue. Simvastatin reduced lung content of the isoprenoid intermediate farnesyl pyrophosphate and decreased RhoA/ROCK signaling in the hypoxia-exposed lung. Preventive or rescue treatment of chronic hypoxia-exposed animals with simvastatin decreased pulmonary vascular resistance, right ventricular hypertrophy, and pulmonary arterial remodeling. Preventive simvastatin treatment improved weight gain, did not lower systemic blood pressure, and did not cause apparent toxic effects on skeletal muscle, liver or brain. Rescue therapy with simvastatin improved exercise capacity. We conclude that simvastatin limits RhoA/ROCK activity in the chronic hypoxia-exposed lung, thus preventing or ameliorating hemodynamic and structural markers of chronic PHT and improving long-term outcome, without causing adverse effects.

chronic lung injury; Rho-kinase; echocardiography; isoprenoid intermediates

PREMATURE BIRTH AND ASSOCIATED chronic lung injury, known as bronchopulmonary dysplasia (BPD), is frequently associated with chronic pulmonary arterial hypertension (PHT) (3). Chronic PHT is characterized by pulmonary arterial remodeling, leading to increased pulmonary arterial pressure, increased pulmonary vascular resistance (PVR), and decreased arterial compliance (4, 11, 62). The normal pulmonary circulation is a low-resistance, high-compliance system suited to accommodate the entire cardiac output. Increased thickening of pulmonary arteries from smooth muscle proliferation and extracellular matrix deposition contributes to decreased pulmonary arterial compliance, increased resistance and increased right ventricle (RV) afterload (36). The RV adapts by undergoing hypertrophy that may be followed by maladaptive chamber dilatation, which precedes RV failure and eventual death (5, 6). Newborns with chronic PHT associated with severe BPD have a high mortality, with one study reporting a 2-year survival rate of 52% (3, 48). Moreover, survivors are at an increased risk for impaired neurological development (34) and recurrence of PHT later in life (58). Currently, there are no treatments of proven efficacy for chronic PHT in neonates.

Previous work from our laboratory has implicated the ras-homolog gene family member A (RhoA)/Rho-kinase (ROCK) signaling pathway in the pathogenesis of experimental chronic neonatal PHT. RhoA/ROCK upregulation leads to increased pulmonary vascular tone and pulmonary arterial remodeling in chronic PHT (66). Treatment with ROCK-specific inhibitors such as fasudil and Y-27632 has been shown to prevent or reverse chronic hypoxic- or bleomycin-induced PHT in neonatal rats (22, 39, 74, 75). In pulmonary artery smooth muscle cells (SMCs), vasoconstriction is regulated by phosphorylation of myosin light chain (MLC) through MLC kinase. Dephosphorylation by MLC phosphatase leads to vasorelaxation (14). ROCK acts by phosphorylating the myosin phosphatase target subunit 1 (MYPT1), which inhibits MLC phosphatase activity, thus favoring a contractile state (59, 66). ROCK mediates arterial remodeling via regulation of antiapoptotic and proproliferative signaling in SMCs and fibroblasts (23, 62, 74). RhoA/ROCK signaling also negatively regulates endothelial nitric oxide synthase (eNOS) function (28, 56).

Statins [3-hydroxy-3-methylglutaryl (HMG)-coenzyme A (CoA) reductase inhibitors] prevent conversion of HMG-CoA to mevalonate, which is the rate-limiting step in cholesterol biosynthesis (15). Inhibition of mevalonate synthesis also decreases the synthesis of isoprenoid intermediates (illustrated in Fig. 1*A*): farnesyl-pyrophosphate (FPP) and geranylgeranyl-pyrophosphate (GGPP) (21). The isoprenoids serve an essential biological role through lipidation of proteins, a process also known as prenylation. Of the isoprenoid intermediates, FPP interacts with the Ras family of proteins while GGPP binds to the Rho family (38). An inactive reservoir of GDP-RhoA remains in the cytosol bound to Rho-specific guanine nucleotide dissociation inhibitor (RhoGDI) (18). GGPP-mediated prenylation of RhoA is required for intracellular cytosolic trafficking and subsequent activation at the membrane (38, 72). Once localized to the membrane, RhoA is activated by guanine nucleotide exchange factors catalyzing the exchange of GDP for GTP. RhoA is inactivated by GTPase-activating proteins

Address for reprint requests and other correspondence: r. P. Jankov, Hospital For Sick Children, 09.9707 Peter Gilgan Centre for Research and Learning, 686 Bay St., Toronto, ON M5G 0A4, Canada (e-mail: robert.jankov@sickkids.ca).

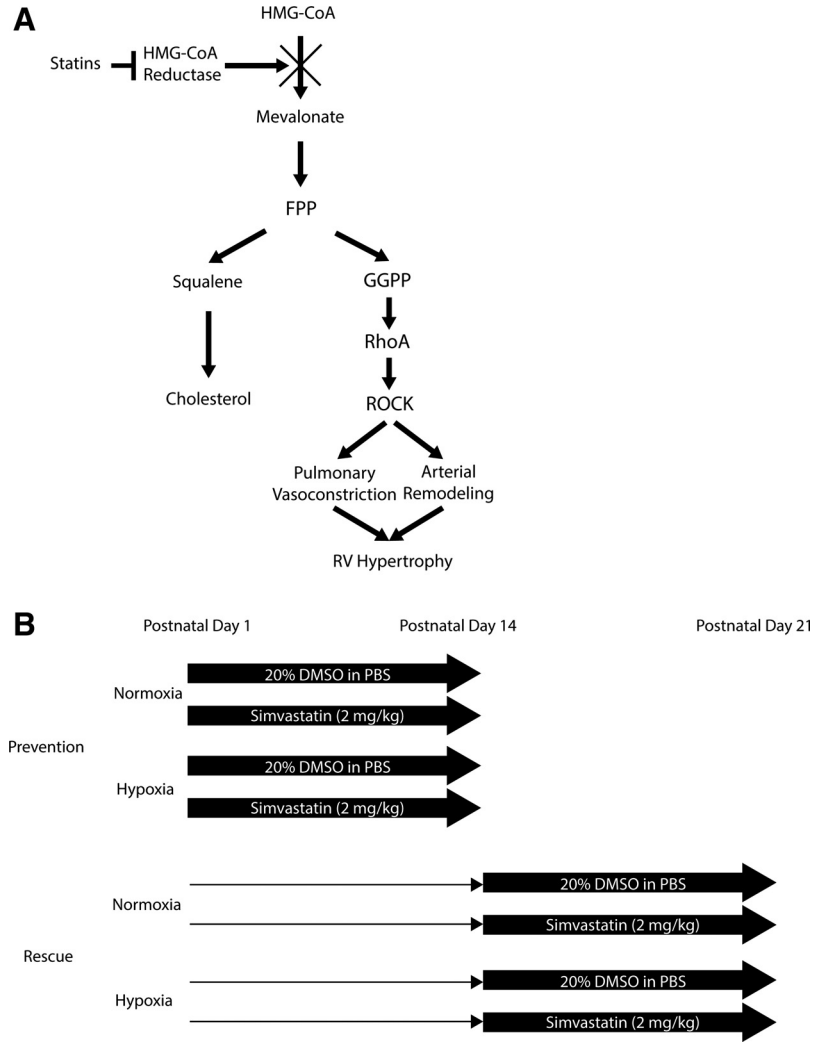

Fig. 1. Illustration of statin inhibition of cholesterol and isoprenoid synthesis pathways. Experimental design for prevention and rescue protocols. *A*: upstream inhibition of HMG-CoA reductase enzyme limits bioavailability of diverging mevalonate products. Reduction of the isoprenoid intermediate geranylgeranyl pyrophosphate (GGPP) limits membrane translocation and activation of RhoA. *B*: overview of the time course and experimental design for prevention and rescue protocols.

through hydrolysis of the phosphate bond (37). GGPP-mediated prenylation of RhoA may also prevent membrane dissociation through the action of RhoGDI, further enhancing RhoA activation (12). Once active, RhoA binds to the Rho-binding domain of ROCK, inducing an active conformational change (65).

Previous work from our laboratory has confirmed the importance of upregulated RhoA activity and its downstream mediator ROCK in the pathogenesis of experimental chronic neonatal lung injury and chronic neonatal PHT (39, 75). Work from other investigators has demonstrated pleiotropic inhibition of RhoA activity by statins (7, 33, 42). Therefore, by limiting the synthesis of GGPP and prenylation of RhoA, statins may reduce pathological RhoA and ROCK activation (72). The objective of this study was to examine the effects of simvastatin in the prevention or rescue of chronic hypoxic PHT in neonatal rats.

MATERIALS AND METHODS

Materials. Simvastatin was from Cayman Chemical (catalog no. 10010344, Ann Arbor, MI). Oxygen-exposure chambers and automated controllers, OxyCycler model A84XOV, were from Biospherix (Parish, NY). Tris-glycine precast gels (catalog no. XP04205BOX, 15 well, 4–20%) and PVDF membranes were from Thermo Scientific (Rockford, IL). Phosphatase and protease inhibitors were from Sigma Life Science (catalog no. P5726-5ML, St. Louis, MO) and Calbiochem (catalog no. 539131-10VL, San Diego, CA), respectively. Acids, alcohols, organic solvents, paraformaldehyde, Permount, and Superfrost/Plus microscope slides were from Fisher Scientific (Whitby, Ontario, Canada). Weigert's resorcin-fuchsin stain was from Rowley Biochemical (catalog no. F-370-1, Danvers, MA). Luxol Fast Blue stain solutions were from Electron Microscopy Sciences (catalog no. 2668101, Hatfield, PA). ELISA kits for alanine transaminase (ALT; catalog no. ab105134), creatine kinase (CK; catalog no. ab155901), high-density lipoprotein (HDL), and low-density/very-low-density lipoprotein (LDL/VLDL) cholesterol (catalog no. ab65390) were purchased from Abcam (Toronto, Ontario, Canada). A free cholesterol assay kit (catalog no. 10007640) was from Cayman Chemical.

Anti-ROCK I (catalog no. SC-5560), anti-cleaved ROCK I (catalog no. SC-52953), anti-glyceraldehyde-3-phosphate dehydrogenase (GAPDH; catalog no. SC-25778) antibodies and protein A/G agarose beads (catalog no. SC-2003) were from Santa Cruz Biotechnology (Santa Cruz, CA). Anti-ROCK II (catalog no. 610624), anti-pan-MYPT1 (catalog no. 612164), and anti-eNOS (catalog on. 61098) were from BD Biosciences (San Jose, CA). Anti-phospho-threonine 850 MYPT1 (catalog no. 36-003) was from Millipore (Etobicoke, Ontario, Canada). Anti-HIF-1α (catalog no. 821503130) was from GeneTex (Irvine, CA). Anti-GTP-RhoA (catalog no. 26904) and anti-RhoA (catalog no. 21017) antibodies were from NewEast Bio-

sciences (King of Prussia, PA). Anti-α-smooth muscle actin antibody (catalog no. MA1-12772) was from Thermo Scientific. Avidin-biotin-peroxidase complex immunohistochemistry kits, 6-diamino-2-phenylindole aqueous mounting medium, and 3,3-diaminobenzidine staining kits were from Vector Laboratories (Burlingame, CA). Goat anti-mouse immunoglobulin (IgG)-peroxidase antibodies, and biotinylated goat anti-mouse IgG (catalog no. 14709) and goat anti-rabbit IgG (catalog no. 14708) were from Cell Signaling Technologies (Beverly, MA).

In vivo experiments. All procedures involving animals were approved by the Animal Care Committee of the Hospital for Sick Children Research Institute and conformed to the guidelines of the Canadian Council on Animal Care. Timed-pregnant Sprague-Dawley rats were from Taconic Farms (Germantown, NY). Commencing on the day after birth [postnatal day (PND) 1], litters of Sprague-Dawley rat pups (equalized sex distribution) were chronically exposed to normobaric hypoxia (13% O_2) or normoxia (21% O_2) until PND 14 (prevention study) or until PND 21 (rescue study). Concurrent with normoxia or hypoxia exposure, rat pups received daily intraperitoneal simvastatin (2 mg/kg) or vehicle (20% DMSO in PBS), from PND 1 to PND 14 (prevention study) or from PND 14 to PND 21 (rescue study). Injury and treatment protocols are illustrated in Fig. 1*B*. Simvastatin was selected as it was the most frequently studied statin in the clinical and experimental PHT literature during the conception of the study design, with a well-defined dose range in neonatal rats (21, 40, 41, 54, 63). Initial dose-response studies (0.1, 2, 5, 10, and 20 mg/kg) were conducted to determine the lowest effective dose in preventing PHT, as guided by echocardiographic estimation of PVR. The highest dose (20 mg/kg) adversely affected weight gain and the lowest dose (0.1 mg/kg) had a minimal effect on PVR (data not shown); therefore 2 mg/kg was the dose chosen for all subsequent studies. Each litter was maintained at $n = 12$ pups, to control for nutritional effects. At the end of each 14- or 21-day exposure period, pups either were killed by pentobarbital overdose or were exsanguinated after anesthesia. Upon completion of the rescue protocol, a subgroup of animals was housed in room air until 10 wk of age for exercise testing.

Simvastatin preparation and delivery. Simvastatin was provided as a crystallized solid and stored in aliquots as a 25 mg/ml solution in DMSO stored at −20°C. Since simvastatin is not soluble in saline, a 0.4 mg/ml solution in 20% DMSO in PBS was heated to 37°C in a temperature regulated shaker just prior to delivery to ensure solubility. Injections were given intraperitoneally (5 μl/g body wt) via a 27-gauge needle, once daily. Vehicle controls received an equivalent volume of 20% DMSO in PBS.

Two-dimensional echocardiography and pulse wave Doppler ultrasound. Two-dimensional echocardiography and pulsed wave Doppler ultrasound was performed as a noninvasive method to assess pulmonary hemodynamics, using a Vivid 7 Advantage (GE Medical Systems, Milwaukee, WI) cardiovascular ultrasound machine with a small high frequency probe (I13L), as previously described (13). Briefly, rat pups were anesthetized with 5% (vol/vol) isoflurane, and the animal was laid supine while spontaneously breathing 2–3% (vol/vol) isoflurane through a modified face mask. A short axis view at the level of the aortic valve was obtained, and the pulmonary artery was identified using color flow Doppler. The pulsed Doppler gate was placed proximal to the pulmonary valve leaflets and aligned with an angle of insonation <20°, maximizing laminar flow. The RV ejection time (RVET) and pulmonary arterial acceleration time (PAAT) were measured using the pulmonary Doppler profile; RVET as the time from onset of systolic flow to completion of systolic flow, and PAAT from onset to peak pulmonary outflow velocity. A surrogate measure of PVR was calculated as a ratio of RVET to PAAT. To determine heart rate, measurements from three intersystolic intervals were averaged to account for beat-to-beat variability. Analyses were undertaken in a blinded fashion using an offline analysis system (ECHOPac, GE Medical Systems).

Right ventricular hypertrophy. Measurement of RV hypertrophy using the Fulton index (RV/LV+S) is a well-established marker of PHT. The heart and lungs were separated, and the atria were removed inferior to the atrioventricular valves. The RV was separated from the left ventricle (LV) and septum. Each component was freeze dried overnight and weighed separately, as previously described (25).

Measurement of systemic blood pressure. Systemic blood pressure was measured noninvasively using a tail cuff Doppler device (LE5002, Harvard Apparatus, Holliston, MA), as previously described (74). Rats were anesthetized with 5% (vol/vol) isoflurane; the animal was laid supine while spontaneously breathing 2–3% (vol/vol) isoflurane through a modified face mask. Due to technical limitations of the device in smaller animals, measurements were carried out between PND 21 and PND 26, as previously described (74).

Exercise tolerance studies. Adult rats (10 wk of age) were trained daily on an Exer-3/6 animal treadmill (Columbus Instruments, Columbus, OH) over a 7-day period. The treadmill speed was initially set to 10 m/min with a 10% uphill incline, and thereafter increased by increments of 2 m/min every 5 min up to a maximum speed of 20 m/min. Distance to fatigue was determined when the rat was unable to maintain pace with the treadmill belt for >3 s, despite encouragement to do so by tapping on the treadmill enclosure (electrical stimuli were not used). Following the 7-day training period, the final testing regimen was as follows: speed of 12.5 m/min for 1 min, followed by 15 m/min for 4 min, 17 m/min for 4 min, and 20 m/min until fatigue. Lowering of the hindquarters and a raised snout, resulting in an altered gait, generally precedes fatigue, which was confirmed by placing the animal on its back and observing a delayed (>2 s) righting reflex. In the case of a normal righting reflex, the test was repeated daily until fatigue was confirmed. Distance covered until fatigue was recorded to the nearest tenth of a meter.

Tissue homogenate preparation. Right lower lobes (6 animals per group, equal sex distribution) were flash frozen, homogenized, and sonicated (40 W for 30 s) in RIPA cell lysis buffer [10 mM $NaPO_4$, 0.3 M NaCl, 0.1% (wt/vol) sodium dodecyl sulfate (SDS), 1% (vol/vol) Nonidet P-40, 1% (vol/vol) sodium deoxycholate, 2 mM EDTA, pH 7.2] containing protease (Calbiochem) and phosphatase (Sigma Life Science) inhibitors. Left lung lobes (6 animals per group, equal sex distribution) were flash frozen, homogenized in lysis buffer (250 mM Tris·HCl, pH 8, 750 mM NaCl, 50 mM $MgCl_2$, 5 mM EDTA, 5% Triton X-100) containing protease and phosphatase inhibitors for immunoprecipitation. The lung homogenates were left on ice for 10 min before centrifugation (8,500 *g* for 10 min). The supernatant was collected and protein concentration was measured by Bradford assay. Samples were stored at −80°C until analysis.

Serum collection. Following euthanasia of animals for tissue collection, the thoracic cavity was exposed and blood was drawn by direct LV cardiac puncture with a 27-gauge needle. Blood was kept at room temperature for 15 min to coagulate in microcentrifuge tubes. The tubes were spun down at 2,000 *g* for 10 min. Supernatant was collected by Pasteur pipette and stored at −80°C until assay.

Western blot analyses. Lung homogenates from six animals per group (equal sex distribution) stored in RIPA buffer containing protease and phosphatase inhibitors. Tissue containing 50–100 μg of protein was boiled for 5 min in SDS sample buffer [60 mM Tris·HCl, 10% (wt/vol) SDS, 5% (vol/vol) glycerol, 2 mM β-mercaptoethanol, pH 6.8] and separated under reducing conditions by SDS polyacrylamide gel electrophoresis for 1–2 h at 100–150 V depending on protein of interest. Following electrophoresis, proteins were transferred to PVDF membranes. All membranes were blocked with 5% BSA for 1 h at room temperature, followed by incubation with primary antibody overnight at 4°C. Blots were then washed with Tris-buffered saline with Tween 20 and placed in secondary antibody for 1 h at room temperature. Following blotting, bands were imaged using an enhanced chemiluminescence kit (SuperSignal West Dura Chemiluminescent Substrate, Thermo Scientific). Dilutions of antibodies were as follows: 1:1,000 for anti-RhoA (21 kDa), anti-cleaved

ROCK I (30 kDa), anti-P-Thr850 MYPT1 (80 kDa), anti-pan MYPT1 (135 kDa), anti-HIF-1α (120 kDa), and anti-eNOS (140 kDa); 1:2,000 for anti-ROCK I (180 kDa) and anti-ROCK II (180 kDa); 1:5,000 for anti-GAPDH (37 kDa); 1:10,000 for secondary antisera.

Blots were electronically captured using a MicroChemi chemiluminescent camera (DNR Bioimaging Systems, Jerusalem, Israel) and quantified by digital densitometry of nonsaturated images with background density removed using ImageJ software (National Institutes of Health, Bethesda, MD). Quantitative analyses were conducted as follows: for each protein of interest, three gels were run comparing all samples from a group (normoxia vehicle, normoxia simvastatin, or hypoxia simvastatin) to all samples from the control group (hypoxia vehicle). Membranes were stripped and then reblotted for the normalizer protein (e.g., pan-MYPT1, RhoA, or GAPDH) to account for differences in protein loading, and results expressed after normalization to the control band, as previously described (24). Representative images show 2 contiguous lanes (the same lanes for the protein of interest and the normalizer) from each group that best represented the quantitative analysis.

RhoA activity assay. The concentration of lung tissue homogenates were equalized to 2 mg/ml in 1 ml lysis buffer. Anti-active RhoA monoclonal antibody (1 μl) was added to the tube followed by 30 μl of resuspended A/G agarose bead slurry. The tubes were incubated at 4°C for 1.5 h with gentle agitation following which beads were pelleted by centrifugation for 2 min at 6,500 *g* at 4°C. The supernatant was removed and stored for measurement of non-GTP-bound RhoA. The beads were washed three times with 0.5 ml 1× lysis buffer, centrifuging, aspirating, and discarding the supernatant each time. After the last wash, all supernatant was removed and discarded. The pellet was resuspended in 20 μl 2× reducing SDS-PAGE sample buffer. Samples were boiled for 5 min then centrifuged for 10 s at 6,500 *g*. Two Western blots were run in parallel with samples from the pellet or the supernatant. The membranes were probed with anti-RhoA primary antibody. The proportion of active RhoA was determined by band densities of active RhoA normalized to total RhoA [GTP-RhoA/(GTP-RhoA+non-GTP-RhoA)].

Histological studies. Two males and two females were randomly selected from each of the experimental groups and euthanized by pentobarbital sodium overdose. Following the opening of the thoracic cavity and trachea cannulation, the pulmonary veins were divided. The pulmonary circulation was flushed with PBS and heparin, to clear the lungs of blood. The lungs were then perfusion fixed with paraformaldehyde while air inflated at a constant pressure (20 cmH_2O). Following dehydration and clearance in xylene, tissues were embedded in paraffin, cut into 5-μm sections, mounted onto Superfrost slides, allowed to air dry, and baked overnight at 43°C. For elastin staining, sections were dewaxed by immersion in xylene, rehydrated in ethanol, rinsed in several washes of distilled water, and then left overnight in Weigert's resorcin-fuchsin stain. For α-smooth muscle actin immunostaining, concentration of primary antibody for α-smooth muscle actin was 1:1,500 and secondary goat anti-mouse antibody was 1:200 then counterstained with Carazzi hematoxylin. Slides were washed in tap water, dehydrated, and mounted with a coverslip using a 70% Permount/30% xylene solution, as previously described (25, 74).

Preparation of cardiac tissue. Paraffin-embedded hearts, cut below the atrioventricular valves and oriented in the short axis, were cut into 5-μm sections and mounted onto Superfrost slides, allowed to air dry, and baked overnight at 43°C. Slides were dewaxed and rehydrated. Sections were stained with hematoxylin, washed in distilled water, and partially dehydrated before counterstaining with eosin. Slides were dehydrated and mounted with a coverslip using a 70% Permount/30% xylene solution. Whole sections were scanned by the Imaging Facility at the Hospital for Sick Children Research Institute, using a 3DHistech Pannoramic 250 Flash II Slide Scanner and Pannoramic Viewer 1.15.4 (3DHISTECH, Budapest, Hungary) software.

Preparation of brain tissue. Paraffin-embedded left brain hemisphere oriented sagitally was cut into 5-μm sections just lateral to the ventricle and mounted onto Superfrost slides, allowed to air dry, and baked overnight at 43°C. Slides were dewaxed and rehydrated. Sections were stained with Luxol fast blue solution (to identify myelin) overnight for 18 h at 56°C, washed in distilled water, placed in lithium carbonate solution for 30 s, and partially dehydrated before counterstaining with cresyl violet blue solution. Slides were dehydrated and mounted with a coverslip using a 70% Permount/30% xylene solution. Whole sections were scanned as described above.

Measurement of percent medial wall area. Percent medial wall area (% MWA) was used as a marker of pulmonary vascular remodeling. Pulmonary arteries (20–100 μm external diameter) were identified on elastin-stained sections by the presence of an inner and outer elastic lamina and proximity to respiratory bronchioles. A minimum of 40 arteries per animal from four unique sections were digitally captured (Pixera Penguin 600CL, San Jose, CA) and analysis was performed in a blinded fashion. Obliquely sectioned vessels where there was a greater than three times difference in perpendicular dimensions, were excluded. Using the "Quick Selection" tool (Adobe Photoshop CS5, Adobe Systems, San Jose, CA), the area of the inner lumen and the whole vessel were outlined and pixel count determined. The following formula was used to determine the % MWA: [(whole vessel area − inner luminal area)/whole vessel area] × 100, as previously described (39).

Evaluation of arterial muscularization. Degree of vessel muscularization was evaluated on sections stained for α-smooth muscle actin. Pulmonary arteries (20–100 μm external diameter and proximity to respiratory bronchioles) were identified on α-smooth muscle actin-immunostained sections. A minimum of 40 arteries per animal from four unique sections were digitally captured and evaluated in a blinded fashion. Degree of muscularization was divided in to three categories: nonmuscular, partially muscular, or fully muscular based on the amount of brown stain surrounding each vessel (none, partially, or completely). Category of muscularity was expressed as a fraction of the total number of vessels examined.

LC-MS/MS. Tissue samples weighing ~200 mg were homogenized (750 mg/3 ml) in 1:1 2-propanol-100 mM ammonium bicarbonate. The equivalent of 225 mg (900 μl of homogenate) was added to a 1.7-ml plastic tube containing internal standards (Sigma-Aldrich, Oakville, Ontario, Canada) and briefly vortexed. A standard curve was generated (0.1–200 ng) for each analyte (mevalonic acid, FPP, and GGPP), treated in the same way as the tissue samples, but with 900 μl of 1:1 2-propanol-100 mM ammonium bicarbonate added instead of sample. Each tube was processed as follows: 900 μl of acetonitrile added, vortexed, chilled on ice, and then centrifuged for 10 min at 4°C at 20,000 *g*. The supernatant was transferred to a clean tube and the pellet was reextracted with 1 ml acetonitrile, vortexed, chilled on ice, and centrifuged for 10 min at 4°C at 20,000 *g*. The supernatants were combined and taken to dryness under a gentle flow of nitrogen gas. The residues were reconstituted in 50 μl of 7:3 methanol-ammonium hydroxide, transferred to 1.5 ml plastic tubes, and centrifuged for 10 min at 4°C at 20,000 *g*. The supernatant was transferred to a 200-μl insert in a 1-ml autosampler vial and injected for LC-MS/MS analysis.

Samples were analyzed by LC-MS/MS using an Agilent 1290 HPLC with QTRAP 5500 mass spectrometer (AB Sciex, Concord, Ontario, Canada) in negative ion mode. One microliter of sample extract was injected into a Kinetex XB-C18 column (50 × 3.0 mm, 2.6 μm, Phenomenex) at a flow rate of 200 μl/min. Mevalonic acid, farnesyl pyrophosphate, and geranylgeranyl pyrophosphate were separated using a gradient of 5 mM ammonium bicarbonate and 0.05% triethylamine in water (MPA) and 5 mM ammonium bicarbonate and 0.05% triethylamine in 80% acetonitrile as follows: starting with 100% MPA, moving to 30% MPA from 0.6 to 4.0 min, then to 0% MPA from 4.0 to 5.0 min, 0% MPA was held from 5.0 to 7.5 min, after 7.5 min the system was returned to 100% MPA and allowed to equilibrate resulting in a total run time of 15 min. The following mass transitions (precursor ion

to the product ion) were monitored for quantification in multiple reaction monitoring mode: mevalonic acid 147 to 59, farnesyl pyrophosphate 381 to 79, and geranylgeranyl pyrophosphate 449 to 79. Data were analyzed and quantified using Analyst Software (AB Sciex).

ELISA. Serum ALT, CK, LDL/VLDL cholesterol and total free cholesterol were measured according to the manufacturer's protocols.

Data presentation and statistical analysis. Values are expressed as means ± SE. Table values are expressed as means ± SD. Analyses were performed using Sigma Plot 12.5 (Systat Software, San Jose, CA). Statistical significance was determined by one-way ANOVA or Kruskal-Wallis ANOVA on ranks for data sets failing a normality test, followed by Student-Newman-Keuls post hoc test where significant ($P < 0.05$) intergroup differences were found.

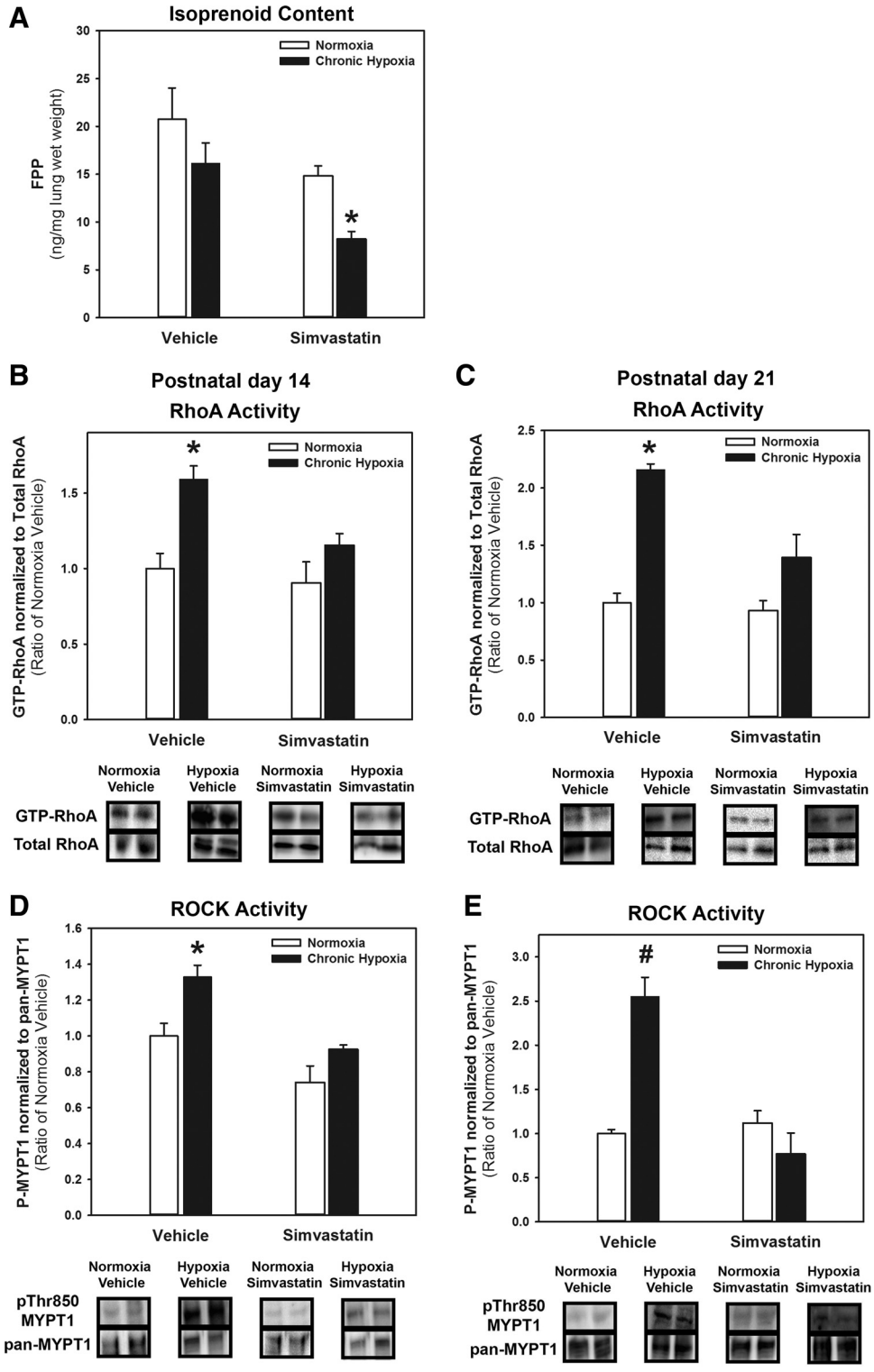

Fig. 2. Simvastatin decreased farnesyl pyrophosphate and RhoA/ROCK activity in the hypoxia-exposed lung. Pups were exposed to chronic hypoxia (13% O_2) or to normoxia (21% O_2) from postnatal day 1 until day 14 (prevention) or day 21 (rescue). Pups were treated by daily intraperitoneal injections of simvastatin (2 mg/kg) or 20% DMSO in PBS (vehicle control) from birth to day 14 (*A*, *B*, and *D*), or from postnatal days 14–21 (*C* and *E*). *A*: FPP lung isoprenoid intermediates analyzed by LC-MS/MS. Western blot analyses of GTP-RhoA normalized to total RhoA (*B* and *C*) and pThr850-MYPT1 normalized to pan-MYPT1 (*D* and *E*). Representative immunoblots are shown below each graph with noncontiguous gel lanes demarcated by black lines. Values represent means ± SE for $n = 5–6$ samples per group. $^*P < 0.05$, by 1-way ANOVA on ranks (*A*) or 1-way ANOVA (*B–D*), compared with all other groups. $\#P < 0.001$, by 1-way ANOVA, compared with all other groups.

RESULTS

Lung FPP content and RhoA/ROCK activity were attenuated by simvastatin. Statins inhibit mevalonate synthesis, which reduces isoprenoid intermediate content (15, 37). As shown in Fig. 2*A*, chronic exposure to hypoxia had no effect on lung FPP content, compared with normoxia-exposed controls. Preventive treatment with simvastatin significantly reduced lung FPP content compared with hypoxia-exposed vehicle-treated pups (Fig. 2*A*). RhoA activity was measured by lung GTP-RhoA content, as a ratio of total (GTP+non-GTP bound) RhoA. Hypoxia-exposed, vehicle-treated pups had significantly elevated RhoA activity in the lung relative to normoxia controls at both PNDs 14 and 21 (Fig. 2, *B* and *C*). Lungs of chronic hypoxia-exposed pups treated with simvastatin had significantly reduced GTP-RhoA content when given as either preventive or as rescue therapy (Figs. 2, *B* and *C*). Lung ROCK activity was determined by pThr850-MYPT1 content, as a ratio of the pan-MYPT1 protein. Lungs of hypoxia-exposed, vehicle-treated pups had significantly increased ROCK activity compared with normoxia controls at both PNDs 14 and 21

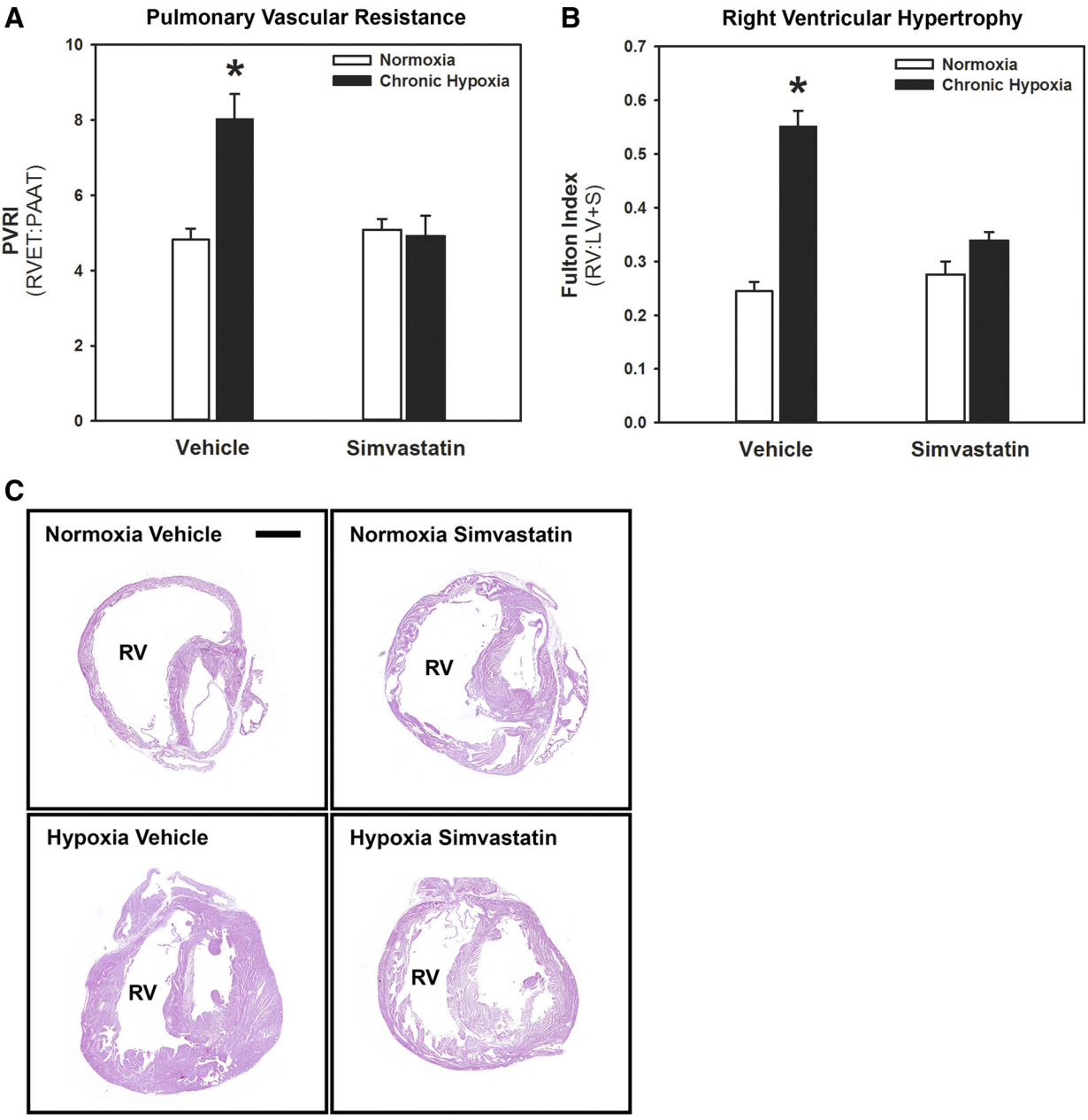

Fig. 3. Simvastatin prevented chronic hypoxia-induced pulmonary hypertension. Pups were exposed to chronic hypoxia (13% O_2) to normoxia (21% O_2) from postnatal day 1 until day 14. Pups were treated by daily intraperitoneal injections of simvastatin (2 mg/kg) or 20% DMSO in PBS (vehicle control). *A*: pulmonary vascular resistance (PVR) index, as measured by the right ventricular ejection time (RVET)-to-pulmonary arterial acceleration time (PAAT) ratio (values represent means ± SE for $n = 8–12$ animals/group). *B*: right ventricle (RV)-to-left ventricle + septum (LV+S) dry weight ratios (Fulton index) as a marker of right ventricular hypertrophy (values represent means ± SE; $n = 7–9$ animals/group). *C*: tiled low-power photomicrographs of hematoxylin and eosin-stained cardiac sections, oriented in the short axis below the atrioventricular valves (RV, right ventricular cavity; scale bar = 2,000 μm), are shown to demonstrate differences in RV free wall thickness between groups. *$P < 0.05$, by 1-way ANOVA on ranks, compared with all other groups.

(Fig. 2, *D* and *E*). Simvastatin significantly attenuated increased lung ROCK activity secondary to hypoxia, relative to the vehicle-treated animals, when given as either preventive or rescue therapy (Fig. 2, *D* and *E*).

Simvastatin prevented chronic PHT. Similar to previous findings (74, 75), exposure to hypoxia significantly increased PVR index (Fig. 3*A*) and Fulton index (Fig. 3*B*) in vehicle-treated animals, compared with normoxia controls. Animals exposed to hypoxia and treated with simvastatin had significantly reduced PVR index (Fig. 3*A*) and Fulton index (Fig. 3*B*) compared with hypoxia-exposed vehicle-treated animals and had values comparable to normoxia controls. % MWA and degree of muscularization were used as measures of pulmonary arterial remodeling. As shown previously (22, 74, 75), and in Fig. 4*A*, pulmonary arteries of animals chronically exposed to hypoxia had greatly increased % MWA, which was accompanied by an increased proportion of fully muscularized arteries (Fig. 4*C*). Treatment with simvastatin reduced both % MWA (Fig. 4*A*) and proportion of fully muscularized arteries (Fig. 4*C*) relative to vehicle-treated controls.

Chronic hypoxia-induced PHT was reversed and exercise capacity increased by rescue treatment with simvastatin. Previous studies have demonstrated that systemic or inhaled treatment with a ROCK inhibitor reversed PHT induced by chronic

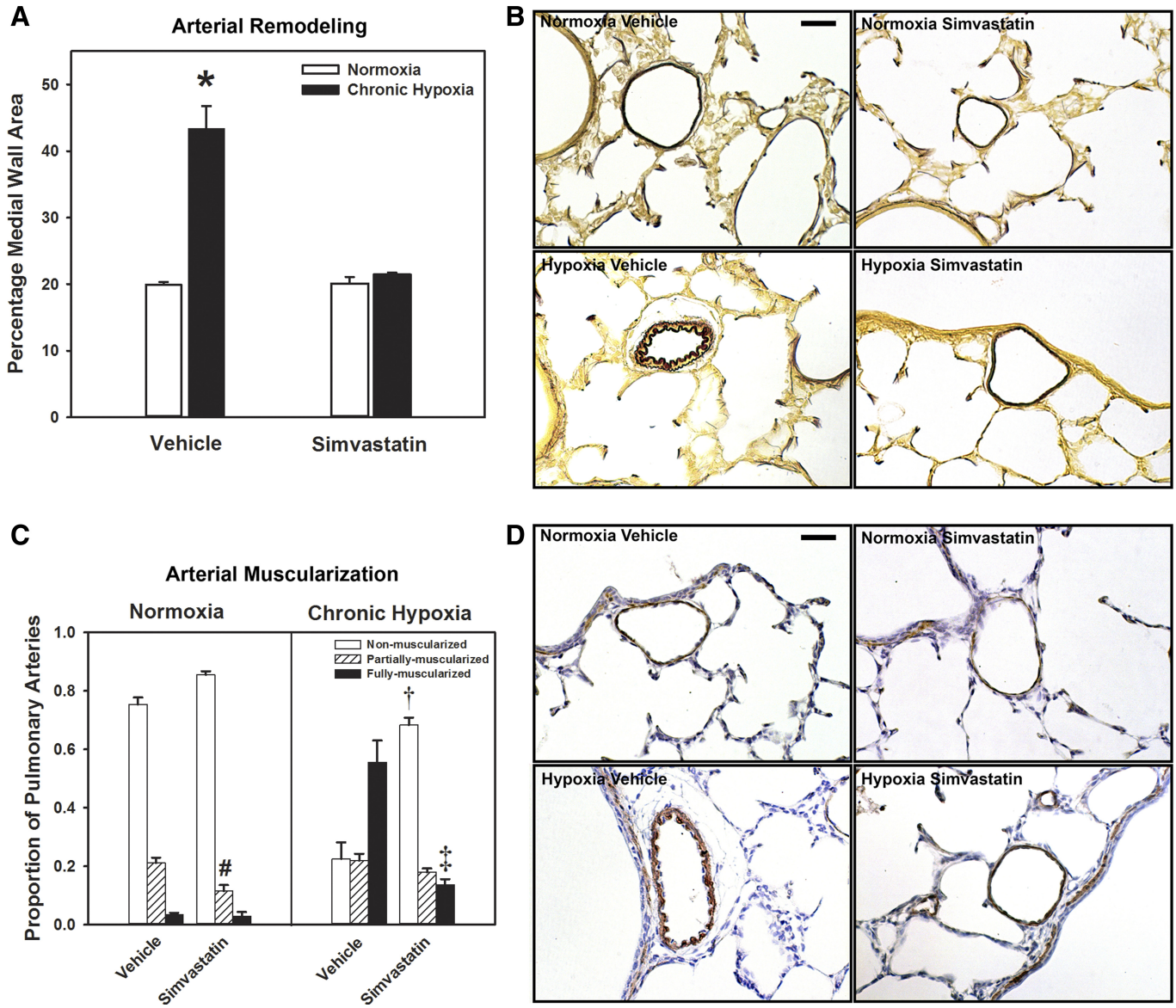

Fig. 4. Simvastatin prevented chronic hypoxia-induced pulmonary arterial remodeling. Pups were exposed to chronic hypoxia (13% O_2) or to normoxia (21% O_2) from postnatal day 1 until day 14. Pups were treated by daily intraperitoneal injections of simvastatin (2 mg/kg) or 20% DMSO in PBS (vehicle control). *A*: percentage arterial medial wall area (values represent means ± SE for $n = 4$ animals/group) as a marker of pulmonary arterial remodeling. *B*: representative photomicrographs of elastin staining (dark brown inner and outer elastic laminae delineating the medial vascular wall; scale bar = 50 μm) demonstrate differences between groups in medial wall thickening. *C*: degree of muscularization (values represent means ± SE for $n = 4$ animals/group) as a marker of pulmonary arterial smooth muscle content. *D*: representative photomicrographs of α-smooth muscle actin staining (dark brown staining surrounding artery; scale bar = 50 μm) demonstrate proliferation of pulmonary arterial smooth muscle. *$P < 0.05$, by 1-way ANOVA on ranks compared with all other groups. #$P < 0.05$, by 1-way ANOVA compared with normoxia vehicle group for proportion of partially muscularized arteries. †$P < 0.001$, by 1-way ANOVA, compared with all other groups for proportions of nonmuscularized and ‡$P < 0.05$ for fully muscularized arteries.

hypoxia in newborn rats (22, 74). Similarly, relative to vehicle-treated animals, sustained rescue treatment with simvastatin significantly decreased PVR (Fig. 5*A*), RV hypertrophy (Fig. 5*B*), % MWA (Fig. 5*C*), and proportion of fully muscularized arteries (Fig. 5*D*) compared with chronic hypoxia-exposed vehicle-treated animals. Exercise capacity in chronic hypoxia, vehicle-treated rats was significantly reduced compared with air-exposed vehicle- or simvastatin-treated controls. Female rats ran a significantly greater distance compared with male rats across all groups and therefore data were stratified by sex.

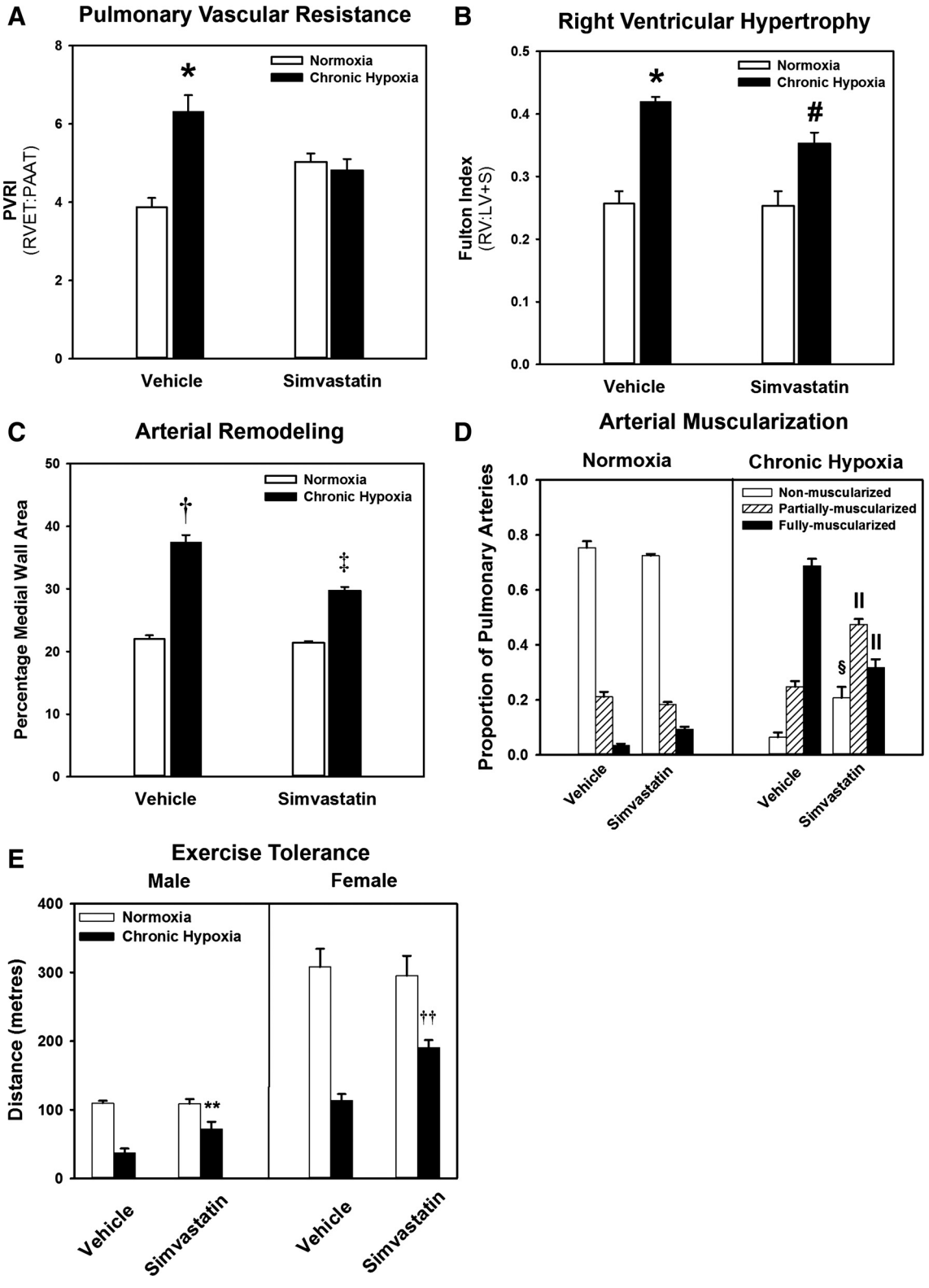

Rescue treatment with simvastatin significantly increased distance run in females and males compared with hypoxia-exposed, vehicle-treated controls (Fig. 5*E*).

Preventive treatment with simvastatin improved hypoxia-induced growth restriction and acute treatment with simvastatin did not affect systemic blood pressure. We have previously reported significant adverse effects of systemic ROCK inhibition, including worsened hypoxia-induced growth restriction and greatly decreased systemic blood pressure (22, 75). As previously documented (75), chronic exposure to hypoxia from birth lead to a significant growth restriction (Fig. 6*A*). Preventive (Fig. 6*A*) treatment with simvastatin increased body weight at PND 14 compared with the hypoxia-exposed, vehicle-treated animals (Fig. 6*A*). Relative to normoxia-exposed controls, chronic hypoxia-exposed animals had significantly increased systolic blood pressure (Fig. 6*B*). Acute treatment with simvastatin had no effect on systolic blood pressure (Fig. 6*B*).

Effects of hypoxia and preventive treatment with simvastatin on brain weight and periventricular myelin content. Relative to normoxia-exposed vehicle-treated animals, chronic exposure to hypoxia significantly decreased brain weight (Fig. 6*C*) and decreased periventricular myelin density (Fig. 6*D*). Treatment with simvastatin had no effects on brain weight in either normoxia- or hypoxia-exposed animals (Fig. 6*C*). Preventive treatment with simvastatin had no effect on periventricular myelin density in normoxia-exposed animals, while causing a significant increase in hypoxia-exposed animals (Fig. 6*D*).

Preventive treatment with simvastatin did not increase serum markers of muscle or liver toxicity. Statin therapy has been reported in adult humans to cause myopathy (increased CK) and liver injury (increased ALT) (8). As shown in Table 1, neither chronic exposure to hypoxia nor treatment with simvastatin altered serum ALT or CK. In addition, no changes in these parameters were observed at 20 $mg \cdot kg^{-1} \cdot day^{-1}$, the highest dose employed in preliminary studies (data not shown).

Preventive treatment with simvastatin had no effect on serum cholesterol. As shown in Table 1, neither chronic exposure to hypoxia nor treatment with simvastatin had any effect on total serum cholesterol. To control for the possible effects of DMSO vehicle on cholesterol levels (16), serum cholesterol was also measured in normoxia- and hypoxia-exposed animals not injected with vehicle. There was no difference in serum cholesterol between noninjected and vehicle-treated groups (data not shown). As shown in Table 1, chronic hypoxia significantly increased serum LDL cholesterol, which was unaffected by treatment with simvastatin.

Effects of hypoxia and preventive treatment with simvastatin on lung cleaved ROCK I, ROCK I, ROCK II, HIF-1α, and eNOS contents. Chronic exposure to hypoxia greatly decreased cleaved ROCK I (constitutively active form of ROCK) content in the lung compared with normoxia-exposed controls (Fig. 7*A*). Normoxia-exposed animals treated with simvastatin had decreased cleaved ROCK I content compared with vehicle-treated animals (Fig. 7*A*). ROCK I content was significantly decreased by exposure to hypoxia, which was unaffected by treatment with simvastatin (Fig. 7*A*). There were no differences in ROCK II content between groups (Fig. 7*C*). HIF-1α is known to be upregulated by hypoxia. Accordingly, neonatal rat pups chronically exposed to hypoxia had significantly increased HIF-1α protein content in the lung compared with normoxia controls (Fig. 7*D*). Treatment with simvastatin had significantly reduced HIF-1α content in lungs exposed to chronic hypoxia (Fig. 7*D*). eNOS expression has been described to be attenuated by increased ROCK activity (64). As shown in Fig. 7*E*, preventive treatment with simvastatin increased eNOS content in both normoxia- and hypoxia-exposed animals.

DISCUSSION

We have previously established a critical role for the ROCK signaling in the pathogenesis of chronic hypoxic PHT in neonatal rats (22, 74, 75). In the present study, we observed that simvastatin both prevented and reversed chronic PHT, at least in part via modulation of RhoA and downstream ROCK activity. The novel aspect of this study was the examination of effects of simvastatin on chronic neonatal PHT. Despite favorable results in adult experimental chronic PHT (21, 44, 52, 63), trials employing statins in human adults with chronic PHT have thus far shown an apparent lack of efficacy (57). The implications of these findings for translation of statins to the neonate remain open, given the potential for maturational differences in response to pharmacological agents that may affect the pulmonary vasculature. For example, selective serotonin reuptake inhibitors (SSRIs) impose a higher risk of PHT in newborns when given to mothers in late pregnancy (9), whereas studies in adults with chronic PHT suggest that SSRIs may improve outcome (30). A small observational study in children with chronic PHT showed improvement in hemodynamic parameters with simvastatin therapy (31). Importantly, the potential utility of statins as a means of targeting RhoA/ROCK activity in the newborn likely extends beyond PHT. We have recently reported a contributory role for upregulated pulmonary ROCK signaling in experimental BPD-like lung

Fig. 5. Simvastatin reversed chronic PHT in juveniles and improved exercise tolerance in young adults. Pups were exposed to chronic hypoxia (13% O_2) or to normoxia (21% O_2) from postnatal day 1 until day 21. Pups were treated by daily intraperitoneal injections of simvastatin (2 mg/kg) or 20% DMSO in PBS (vehicle control) from postnatal days 14 to 21. *A*: pulmonary vascular resistance index (PVRI), as measured by the right ventricular ejection time (RVET)-to-pulmonary arterial acceleration time (PAAT) ratio (values represent means ± SE for $n = 10$ animals/group). *B*: right ventricle (RV)-to-left ventricle + septum (LV+S) dry weight ratios (Fulton index) as a marker of right ventricular hypertrophy (values represent means ± SE $n = 7$–9 animals/group). *C*: percentage arterial medial wall area (values represent means ± SE for $n = 4$ animals/group) as a marker of pulmonary arterial remodeling. *D*: degree of muscularization (values represent means ± SE for $n = 4$ animals/group) as a marker of pulmonary arterial smooth muscle content. *E*: maximum exercise capacity measured in meters run (values represent means ± SE for $n = 5$–8 animals/group). *$P < 0.05$, by 1-way ANOVA on ranks, compared with all other groups. #$P < 0.05$, by 1-way ANOVA on ranks, compared with normoxia-exposed groups. †$P < 0.05$, by 1-way ANOVA, compared with all other groups, ‡$P < 0.05$, by 1-way ANOVA, compared with normoxia-exposed groups. §$P < 0.05$ (nonmuscularized arteries), ‖$P < 0.001$ (fully muscularized and partially muscularized arteries), by 1-way ANOVA, compared with hypoxia vehicle group. **$P < 0.05$, by 1-way ANOVA, compared with hypoxia vehicle group of the same sex. ††$P < 0.001$, by 1-way ANOVA, compared with hypoxia vehicle group of the same sex.

injury (39), a developmental lung disorder of prematurity characterized by inhibited pulmonary angiogenesis and alveologenesis. Similarly, pulmonary hypoplasia and vascular remodeling in fetal rats with nitrofen-induced congenital diaphragmatic hernia (CDH), in which RhoA may play a pathological role (67), was ameliorated by maternally administered simvastatin (45). As there are currently no effective preventive therapies for developmental lung disorders such and BPD and

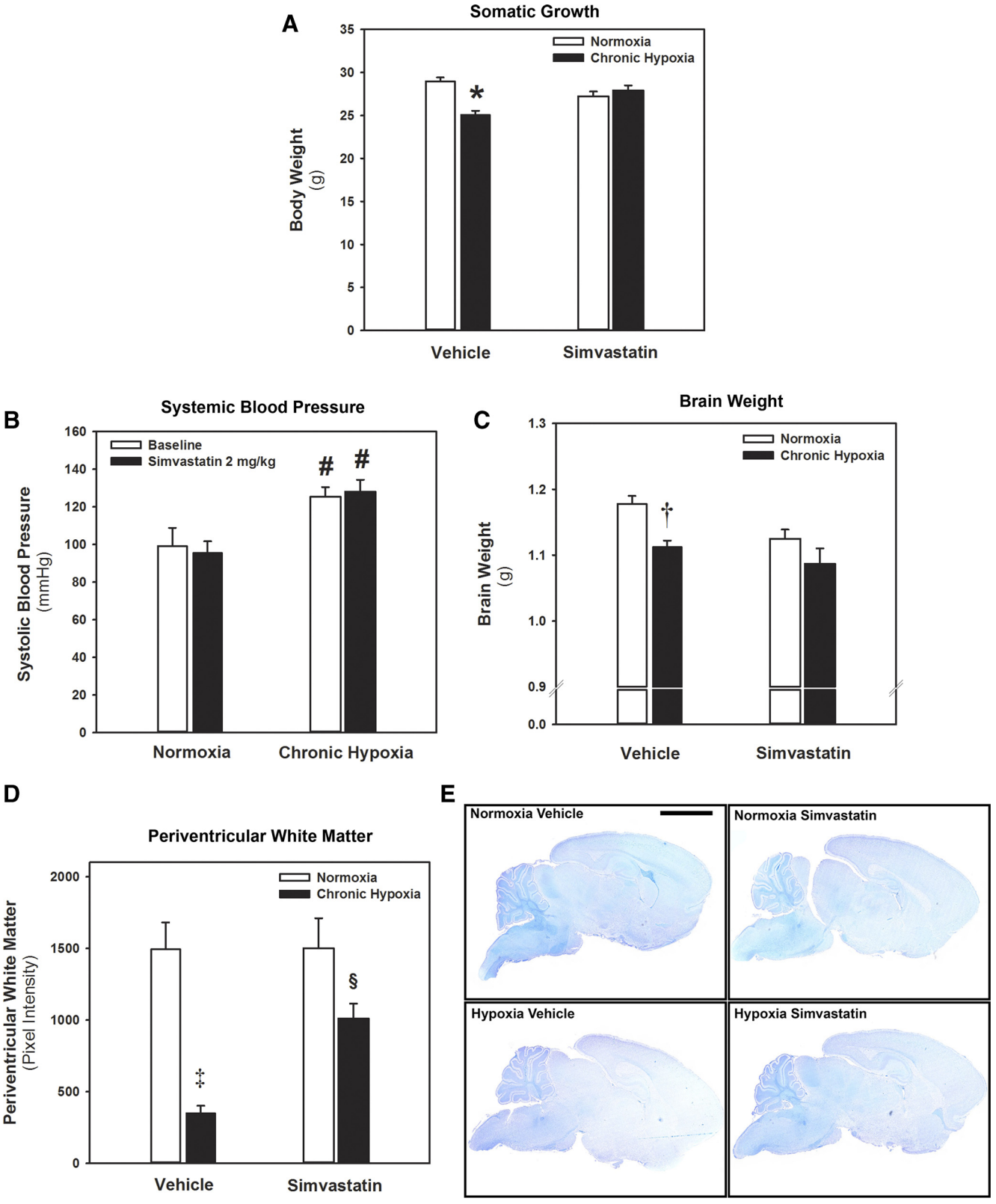

Table 1. *Effects of preventative treatment with simvastatin (2 mg·kg^{-1}·day^{-1}) on serum markers of toxicity*

Serum Analyte	Normoxia Vehicle	Normoxia Simvastatin	Hypoxia Vehicle	Hypoxia Simvastatin
ALT, μmol/ml	1.112 ± 0.276	1.277 ± 0.242	1.126 ± 0.271	1.373 ± 0.407
CK, μmol/ml	10.169 ± 0.774	10.328 ± 1.261	10.66 ± 0.483	10.811 ± 0.286
Total cholesterol, mg/dl	447.44 ± 108.63	537.524 ± 125.892	499.514 ± 115.439	439.539 ± 109.911
LDL cholesterol, mg/dl	273.112 ± 49.38	252.61 ± 38.923	387.556 ± 103.269*	362.039 ± 53.775#

Values represent means ± SD for $n = 6$ animals per group. *$P < 0.05$, by 1-way ANOVA, compared to both Normoxia groups. #$P < 0.05$, by 1-way ANOVA, compared to Normoxia Simvastatin group.

CDH, or to prevent or rescue chronic PHT in neonates (26), these findings point toward statins as a potentially useful therapy. We evaluated dose-response effects of simvastatin, establishing a dose that balanced efficacy and safety. This aspect is critical for potential translation since therapies designed to ameliorate injury to the lung and pulmonary vasculature could have unanticipated adverse effects on other systems, particularly the developing brain. Collectively, our findings provide compelling initial evidence for the translational potential of statin therapy for neonatal pulmonary disease.

We observed that preventively administered simvastatin attenuated the activity of RhoA, normalized PVR, and reduced both RV and pulmonary arterial structural remodeling. In our rescue protocol, the reduction of RhoA/ROCK activity also reduced PVR and led to significant but incomplete reversal of cardiac and vascular remodeling. Severity of pulmonary vascular changes secondary to chronic hypoxia peaks by 14 days of exposure and is stable from days 14 to 21; therefore, effects of rescue therapies (given from days 14 to 21) reflect reversal rather than slowed progression of injury. Rats exposed to chronic hypoxia receiving rescue treatment with simvastatin also had improved exercise capacity as young adults in keeping with an important and relevant functional improvement.

The isoprenoid GGPP contributes to the pathogenesis of PHT by prenylation-mediated intracellular trafficking and membrane localization, and subsequent activation of RhoA (21, 47, 60, 72). In the present study, we observed an increase in FPP and in HIF-1α content in the lungs of chronic hypoxia-exposed rats. We also observed that simvastatin reduced lung content of FPP in hypoxia-exposed animals, with a trend toward reduction in normoxia controls. Presumably, a reduction of FPP also led to decreased GGPP as indicated by reduced RhoA activity; however, we were unable to reliably measure GGPP content in lung. It is known that HIF-1α activity is elevated in hypoxia, which in turn increases transcription of RhoA and/or ROCK (53). Treatment with simvastatin decreased pulmonary HIF-1α levels in chronic hypoxia-exposed animals but did not affect lung content of RhoA or of either ROCK isoform (20, 69). Therefore, the effect of simvastatin could be largely attributed to downregulation of RhoA activity via inhibition of isoprenoid intermediates, rather than by changes in protein content mediated by HIF-1α. In support of this observation, Girgis and colleagues (21) demonstrated that concurrent supplementation of mevalonate with simvastatin treatment negated any beneficial effects in experimental PHT.

The pathology of chronic hypoxic PHT is characterized in neonatal animals by severe pulmonary vascular remodeling (71). In previous studies, inhibition of ROCK signaling prevented vascular remodeling by inhibiting SMC proliferation (75). Rescue therapy with ROCK inhibitor opposed the anti-apoptotic effect of ROCK (specifically by ROCK II), therefore stimulating SMC apoptosis and leading to reversal of remodeling (74). Inhibited NO-cGMP signaling plays a major role in the pathogenesis of chronic PHT (32, 49). ROCK inhibits eNOS activity and disrupts the stability of eNOS mRNA, thus reducing NO bioavailability (17, 28). In the present study, we observed that simvastatin increased eNOS content, which further supports suppression of ROCK activity as a major mechanism for simvastatin effects on chronic neonatal PHT (35).

Neonates are particularly susceptible to adverse and off-target effects of pharmacological agents (2). Documented adverse effects of statins in adult humans include hepatic injury and muscle pain. In rabbits, high-dose simvastatin (50 mg·kg^{-1}·day^{-1}) increased serum lactate dehydrogenase, CK, and ALT (27). In the present study, we did not observe any significant increase in serum levels of ALT or CK, even at doses of simvastatin as high as 20 mg/kg. Systemically administered ROCK inhibitors restrict somatic growth, thus limiting translational potential to the neonate (75). In the present study, simvastatin did not adversely affect somatic growth in normoxia-exposed animals and actually restored normal growth in chronic hypoxia-exposed animals. In addition, simvastatin did not affect systolic blood pressure, unlike systemic ROCK inhibitors (22). We did not examine effects of exposure to hypoxia or of simvastatin therapy on RhoA/ROCK activity in systemic vessels, but we speculate that a lack of effect of simvastatin on systemic vascular tone reflects a greater hypoxia-induced upregulation of RhoA/ROCK activity in the pulmonary, compared with the systemic, vasculature.

The usual target of statin therapy is a reduction in serum cholesterol, which in the neonate may represent an adverse

Fig. 6. Effects of chronic hypoxia from birth and preventive simvastatin treatment on somatic and brain growth, brain myelination, and systemic blood pressure. Pups were exposed to chronic hypoxia (13% O_2) or to normoxia (21% O_2) from postnatal day 1 until day 14. Pups were treated by daily intraperitoneal injections of simvastatin (2 mg/kg) or 20% DMSO in PBS (vehicle control). *A*: body weight. Values represent means ± SE for $n = 10$–12 animals per group. *B*: systemic blood pressure following therapy with simvastatin. Values represent means ± SE for $n = 6$ animals per group. *C*: brain weight. Values represent means ± SE for $n = 6$ samples per group. *D*: myelin pixel density. Values represent means ± SE for $n = 4$ samples per group. *E*: tiled low-power representative photomicrographs of Luxol fast blue staining on sagittal brain sections (myelin = dark blue stain; scale bar = 2,500 μm). *$P < 0.05$, by 1-way ANOVA, compared with all other groups. #$P < 0.05$, by 1-way ANOVA, compared with normoxia controls. †$P < 0.05$, by 1-way ANOVA, compared with normoxia vehicle. ‡$P < 0.001$, by 1-way ANOVA, compared with normoxia controls. §$P < 0.05$, by 1-way ANOVA, compared with hypoxia vehicle group.

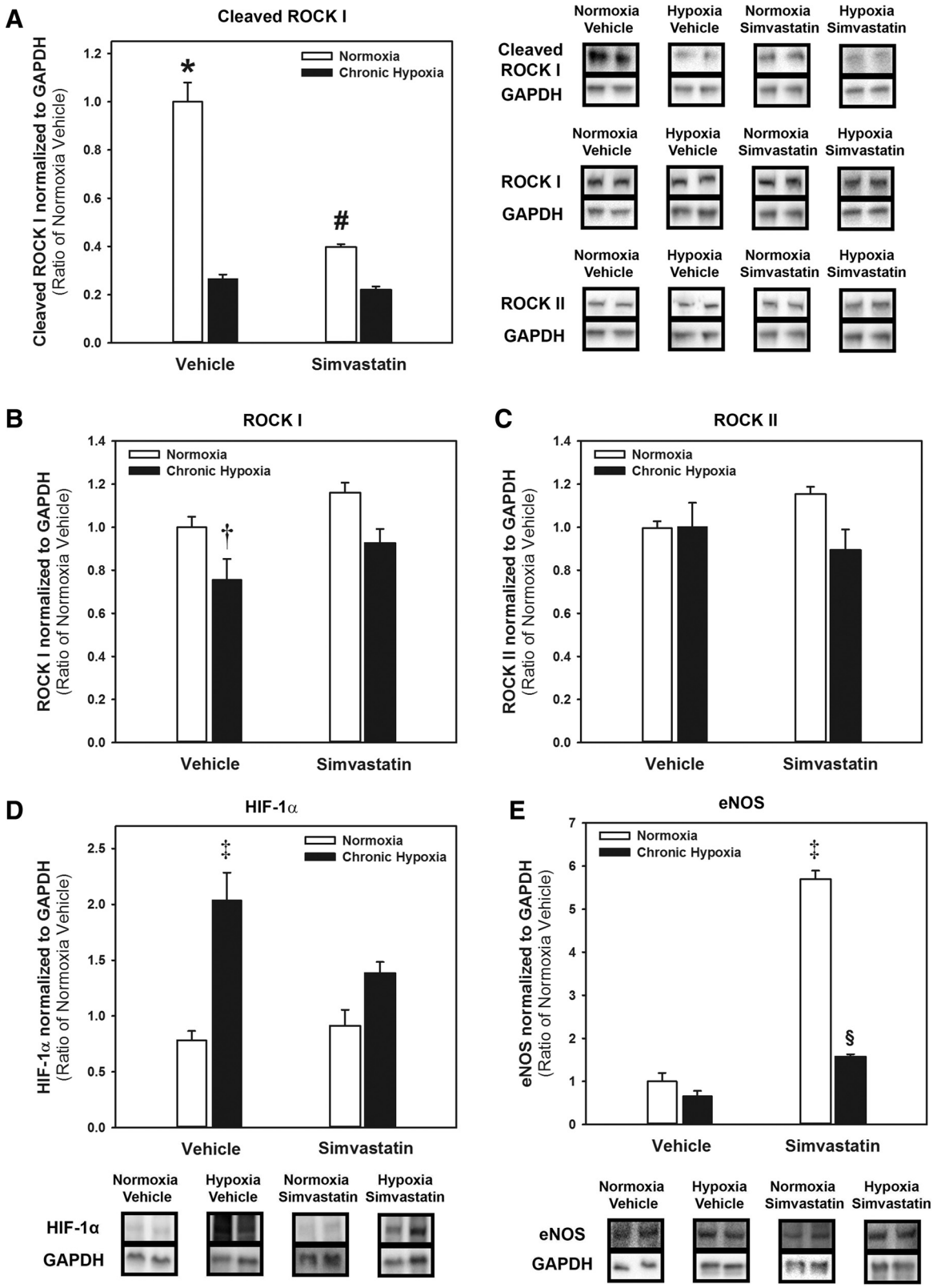

Fig. 7. Effects of preventive simvastatin on lung cleaved ROCK I, ROCK I, ROCK II, HIF-1α, and eNOS content. Pups were exposed to chronic hypoxia (13% O_2) or to normoxia (21% O_2) from postnatal day 1 until day 14. Pups were treated by daily intraperitoneal injections of simvastatin (2 mg/kg) or 20% DMSO in PBS (vehicle control). Western blot analyses for cleaved ROCK I (*A*), ROCK I (*B*), ROCK II (*C*), HIF-1α (*D*), and eNOS (*E*), all normalized to GAPDH. Representative immunoblots are shown with noncontiguous gel lanes demarcated by black lines. Values represent means ± SE for $n = 5–6$ samples per group. *$P < 0.05$, by 1-way ANOVA on ranks, compared with all other groups. #$P < 0.05$, by 1-way ANOVA on ranks, compared with hypoxia simvastatin group. †$P < 0.05$, by 1-way ANOVA, compared with normoxia simvastatin group. ‡$P < 0.001$, by 1-way ANOVA, compared with all other groups. §$P < 0.05$, by 1-way ANOVA, compared with hypoxia vehicle group.

effect, given the reliance of the developing brain on cholesterol for normal development (55). Interestingly, neither simvastatin nor the DMSO vehicle altered total serum cholesterol levels or LDL cholesterol in the newborn rat. This finding is likely explained by the fact that breastfeeding neonates rely less on endogenous synthesis of cholesterol to maintain serum levels, due to the presence of high levels of cholesterol in breast milk (19). Indeed, high doses of statins have not been found to alter brain cholesterol levels, which is required for myelin formation (1, 10, 46, 68). Lipid soluble statins such as simvastatin can cross the blood-brain barrier by lactonization. However, statins do not accumulate in the brain, being rapidly eliminated by the P-glycoprotein transporter (51). Furthermore, CYP3A4, the enzyme responsible for simvastatin metabolism and activation, is absent from the rodent brain (61, 68) and has only been detected in the human brain at one-tenth the level of liver CYP3A4 (73). Prematurely born humans have an increased risk for long-term neurodevelopmental disability. In models of newborn neurological injury and abnormal development, statins prevented injury through modulation of inflammation, leading to normalized morphology, white matter content, and brain weight (43, 54, 70). While there were no reported adverse effects from simvastatin in a small observational study in children with PHT, further study is needed to assess safety and efficacy in the newborn population despite our present reassuring findings (31).

There are a number of limitations to this study. First, our chronic hypoxia model of PHT does not mimic chronic PHT secondary to developmental lung disorders, such as BPD, which is among the most common causes of chronic PHT in neonates and infants (26). Therefore, effects of statin therapy should be studied in models mimicking inhibited pulmonary angiogenesis and arrested lung development, as observed in BPD (50). Second, use of simvastatin as a rescue therapy showed incomplete effects compared with prevention, which may have been overcome by prolongation of therapy. Third, we did not conduct functional neurological examination to substantiate our morphological findings suggesting an improvement in hypoxia-mediated disruption of myelination with simvastatin treatment. Fourth, our focus was restricted to the activity of RhoA. Many other GTPase proteins could be similarly affected by statin therapy, based on their dependence for prenylation-mediated activation. Of note, the Ras family of G proteins and other members of the Rho family such as Rac1 and Cdc42 may warrant further investigation since they are known to be involved in cardiac hypertrophy, actin cytoskeleton remodeling, and SMC proliferation (29, 65). Lastly, evaluation of sex differences in response to therapy is a relevant biological variable that should be evaluated in future studies.

In summary, simvastatin-mediated inhibition of isoprenoid intermediates downregulates RhoA activity, leading to prevention and reversal of chronic PHT. Our findings suggest that simvastatin was well tolerated, lacked apparent adverse systemic or neurological effects, and therefore holds promise as a potentially translatable means of limiting pathological ROCK activity in the neonate.

ACKNOWLEDGMENTS

The authors thank Denis Reynaud and Ashley St. Pierre of the Analytical Facility for Bioactive Molecules, The Hospital for Sick Children, Toronto, Canada, for assistance with LC- 550 MS/MS analysis of lung tissue isoprenoid intermediates.

GRANTS

This work was supported by operating funding from the Canadian Institutes of Health Research (CIHR; MOP-84290 to R. P. Jankov) and by infrastructure funding from the Canada Foundation for Innovation (to R. P. Jankov). A. Jain was supported by a Clinician-Scientist Training Program Award from the Hospital for Sick Children Research Training Centre and by a Queen Elizabeth II/Heart and Stroke Foundation of Ontario Graduate Scholarship in Science and Technology. M. J. Wong was supported by a Graduate Scholarship from the Department of Physiology, University of Toronto and by a Lorne Phenix Graduate award from the Cardiovascular Sciences Collaborative Program, Faculty of Medicine, University of Toronto.

DISCLOSURES

No conflicts of interest, financial or otherwise, are declared by the author(s).

AUTHOR CONTRIBUTIONS

M.J.W. and R.P.J. conceived and designed research; M.J.W., C.K., J.I., A.J., and R.P.J. performed experiments; M.J.W., A.J., and R.P.J. analyzed data; M.J.W. and R.P.J. interpreted results of experiments; M.J.W. and R.P.J. prepared figures; M.J.W. and R.P.J. drafted manuscript; M.J.W., C.K., J.I., A.J., and R.P.J. edited and revised manuscript; M.J.W., C.K., J.I., A.J., and R.P.J. approved final version of manuscript.

REFERENCES

1. **Adibhatla RM, Hatcher JF.** Altered lipid metabolism in brain injury and disorders. *Subcell Biochem* 49: 241–268, 2008.
2. **Allegaert K, van den Anker J.** Neonatal drug therapy: the first frontier of therapeutics for children. *Clin Pharmacol Ther* 98: 288–297, 2015.
3. **Ambalavanan N, Mourani P.** Pulmonary hypertension in bronchopulmonary dysplasia. *Birth Defects Res A Clin Mol Teratol* 100: 240–246, 2014.
4. **Bhat R, Salas AA, Foster C, Carlo WA, Ambalavanan N.** Prospective analysis of pulmonary hypertension in extremely low birth weight infants. *Pediatrics* 129: e682–e689, 2012.
5. **Bogaard HJ, Abe K, Vonk Noordegraaf A, Voelkel NF.** The right ventricle under pressure: cellular and molecular mechanisms of right-heart failure in pulmonary hypertension. *Chest* 135: 794–804, 2009.
6. **Bronicki RA, Baden HP.** Pathophysiology of right ventricular failure in pulmonary hypertension. *Pediatr Crit Care Med* 11, *Suppl* 2: S15–S22, 2010.
7. **Bulhak A, Roy J, Hedin U, Sjoquist PO, Pernow J.** Cardioprotective effect of rosuvastatin in vivo is dependent on inhibition of geranylgeranyl pyrophosphate and altered RhoA membrane translocation. *Am J Physiol Heart Circ Physiol* 292: H3158–H3163, 2007.
8. **Chaipichit N, Krska J, Pratipanawatr T, Jarernsiripornkul N.** Statin adverse effects: patients' experiences and laboratory monitoring of muscle and liver injuries. *Int J Clin Pharm* 37: 355–364, 2015.
9. **Chambers CD, Hernandez-Diaz S, Van Marter LJ, Werler MM, Louik C, Jones KL, Mitchell AA.** Selective serotonin-reuptake inhibitors and risk of persistent pulmonary hypertension of the newborn. *N Engl J Med* 354: 579–587, 2006.
10. **Dietschy JM.** Central nervous system: cholesterol turnover, brain development and neurodegeneration. *Biol Chem* 390: 287–293, 2009.
11. **Donti A, Formigari R, Ragni L, Manes A, Galie N, Picchio FM.** Pulmonary arterial hypertension in the pediatric age. *J Cardiovasc Med* 8: 72–77, 2007.
12. **Dransart E, Olofsson B, Cherfils J.** RhoGDIs revisited: novel roles in Rho regulation. *Traffic* 6: 957–966, 2005.
13. **Dunlop K, Gosal K, Kantores C, Ivanovska J, Dhaliwal R, Desjardins JF, Connelly KA, Jain A, McNamara PJ, Jankov RP.** Therapeutic hypercapnia prevents inhaled nitric oxide-induced right-ventricular systolic dysfunction in juvenile rats. *Free Radic Biol Med* 69C: 35–49, 2014.
14. **Duong-Quy S, Bei Y, Liu Z, Dinh-Xuan AT.** Role of Rho-kinase and its inhibitors in pulmonary hypertension. *Pharmacol Ther* 137: 352–364, 2013.
15. **Endo A.** A historical perspective on the discovery of statins. *Proc Jpn Acad Ser B Phys Biol Sci* 86: 484–493, 2010.

16. **Fani K, Debons AF, Jimenez FA, Hoover EL.** Cholesterol-induced atherosclerosis in the rabbit: effect of dimethyl sulfoxide on existing lesions. *J Pharmacol Exp Ther* 244: 1145–1149, 1988.
17. **Farrow KN, Lakshminrusimha S, Reda WJ, Wedgwood S, Czech L, Gugino SF, Davis JM, Russell JA, Steinhorn RH.** Superoxide dismutase restores eNOS expression and function in resistance pulmonary arteries from neonatal lambs with persistent pulmonary hypertension. *Am J Physiol Lung Cell Mol Physiol* 295: L979–L987, 2008.
18. **Garcia-Mata R, Boulter E, Burridge K.** The 'invisible hand': regulation of Rho GTPases by RhoGDIs. *Nat Rev Mol Cell Biol* 12: 493–504, 2011.
19. **Garcia C, Duan RD, Brevaut-Malaty V, Gire C, Millet V, Simeoni U, Bernard M, Armand M.** Bioactive compounds in human milk and intestinal health and maturity in preterm newborn: an overview. *Cell Mol Biol* 59: 108–131, 2013.
20. **Gilkes DM, Xiang L, Lee SJ, Chaturvedi P, Hubbi ME, Wirtz D, Semenza GL.** Hypoxia-inducible factors mediate coordinated RhoA-ROCK1 expression and signaling in breast cancer cells. *Proc Natl Acad Sci USA* 111: E384–E393, 2014.
21. **Girgis RE, Mozammel S, Champion HC, Li D, Peng X, Shimoda L, Tuder RM, Johns RA, Hassoun PM.** Regression of chronic hypoxic pulmonary hypertension by simvastatin. *Am J Physiol Lung Cell Mol Physiol* 292: L1105–L1110, 2007.
22. **Gosal K, Dunlop K, Dhaliwal R, Ivanovska J, Kantores C, Desjardins JF, Connelly KA, McNamara PJ, Jain A, Jankov RP.** Rho-kinase mediates right ventricular systolic dysfunction in rats with chronic neonatal pulmonary hypertension. *Am J Respir Cell Mol Biol* 52: 717–727, 2015.
23. **Gosal K, Dunlop K, Dhaliwal R, Ivanovska J, Kantores C, Desjardins JF, Connelly KA, McNamara PJ, Jain A, Jankov RP.** Rho-kinase mediates right ventricular systolic dysfunction in rats with chronic neonatal pulmonary hypertension. *Am J Respir Cell Mol Biol* 52: 717–727, 2015.

23a.(a)**Guignabert C, Tu L, Girerd B, Ricard N, Huertas A, Montani D, Humbert M.** New molecular targets of pulmonary vascular remodeling in pulmonary arterial hypertension: importance of endothelial communication. *Chest* 147: 529–537, 2015.

24. **Jankov RP, Kantores C, Belcastro R, Yi S, Ridsdale RA, Post M, Tanswell AK.** A role for platelet-derived growth factor β-receptor in a newborn rat model of endothelin-mediated pulmonary vascular remodeling. *Am J Physiol Lung Cell Mol Physiol* 288: L1162–L1170, 2005.
25. **Jankov RP, Luo X, Cabacungan J, Belcastro R, Frndova H, Lye SJ, Tanswell AK.** Endothelin-1 and O_2-mediated pulmonary hypertension in neonatal rats: a role for products of lipid peroxidation. *Pediatr Res* 48: 289–298, 2000.
26. **Jankov RP, Tanswell AK.** Chronic neonatal lung injury and care strategies to decrease injury. In: *Fetal and Neonatal Lung Development: Clinical Correlates and Technologies for the Future*, edited by Jobe A, Whitsett JA, Abman SH. New York: Cambridge University Press, 2016, p. 205–222.
27. **Jasinska M, Owczarek J, Orszulak-Michalak D.** The influence of simvastatin at high dose and diltiazem on myocardium in rabbits, the biochemical study. *Acta Pol Pharm* 63: 386–390, 2006.
28. **Kato M, Blanton R, Wang GR, Judson TJ, Abe Y, Myoishi M, Karas RH, Mendelsohn ME.** Direct binding and regulation of RhoA protein by cyclic GMP-dependent protein kinase Ialpha. *J Biol Chem* 287: 41342–41351, 2012.
29. **Kavalipati N, Shah J, Ramakrishan A, Vasnawala H.** Pleiotropic effects of statins. *Indian J Endocrinol Metab* 19: 554–562, 2015.
30. **Kawut SM, Horn EM, Berekashvili KK, Lederer DJ, Widlitz AC, Rosenzweig EB, Barst RJ.** Selective serotonin reuptake inhibitor use and outcomes in pulmonary arterial hypertension. *Pulm Pharmacol Ther* 19: 370–374, 2006.
31. **King WT, Day RW.** Treatment of pediatric pulmonary hypertension with simvastatin: an observational study. *Pediatr Pulmonol* 46: 261–265, 2011.
32. **Klinger JR, Abman SH, Gladwin MT.** Nitric oxide deficiency and endothelial dysfunction in pulmonary arterial hypertension. *Am J Respir Crit Care Med* 188: 639–646, 2013.
33. **Kolavennu V, Zeng L, Peng H, Wang Y, Danesh FR.** Targeting of RhoA/ROCK signaling ameliorates progression of diabetic nephropathy independent of glucose control. *Diabetes* 57: 714–723, 2008.
34. **Konduri GG, Vohr B, Robertson C, Sokol GM, Solimano A, Singer J, Ehrenkranz RA, Singhal N, Wright LL, Van Meurs K, Stork E, Kirpalani H, Peliowski A, Johnson Y.** Early inhaled nitric oxide therapy for term and near-term newborn infants with hypoxic respiratory failure: neurodevelopmental follow-up. *J Pediatr* 150: 235–240, 2007.
35. **Kosmidou I, Moore JP, Weber M, Searles CD.** Statin treatment and 3′ polyadenylation of eNOS mRNA. *Arterioscler Thromb Vasc Biol* 27: 2642–2649, 2007.
36. **Lankhaar JW, Westerhof N, Faes TJ, Gan CT, Marques KM, Boonstra A, van den Berg FG, Postmus PE, Vonk-Noordegraaf A.** Pulmonary vascular resistance and compliance stay inversely related during treatment of pulmonary hypertension. *Eur Heart J* 29: 1688–1695, 2008.
37. **Laufs U, Liao JK.** Direct vascular effects of HMG-CoA reductase inhibitors. *Trends Cardiovasc Med* 10: 143–148, 2000.
38. **Laufs U, Liao JK.** Post-transcriptional regulation of endothelial nitric oxide synthase mRNA stability by Rho GTPase. *J Biol Chem* 273: 24266–24271, 1998.
39. **Lee AH, Dhaliwal R, Kantores C, Ivanovska J, Gosal K, McNamara PJ, Letarte M, Jankov RP.** Rho-kinase inhibitor prevents bleomycin-induced injury in neonatal rats independent of effects on lung inflammation. *Am J Respir Cell Mol Biol* 50: 61–73, 2014.
40. **Lee YH, Kim KC, Cho MS, Hong YM.** Changes of pulmonary pathology and gene expressions after simvastatin treatment in the monocrotaline-induced pulmonary hypertension rat model. *Korean Circ J* 41: 518–527, 2011.
41. **Li A, Lv S, Yu Z, Zhang Y, Ma H, Zhao H, Piao H, Li S, Zhang N, Sun C.** Simvastatin attenuates hypomyelination induced by hypoxia-ischemia in neonatal rats. *Neurol Res* 32: 945–952, 2010.
42. **Li M, Li Z, Sun X.** Statins suppress MMP2 secretion via inactivation of RhoA/ROCK pathway in pulmonary vascular smooth muscles cells. *Eur J Pharmacol* 591: 219–223, 2008.
43. **Ling Q, Tejada-Simon MV.** Statins and the brain: new perspective for old drugs. *Prog Neuropsychopharmacol Biol Psychiatry* 66: 80–86, 2015.
44. **Liu ZQ, Liu B, Yu L, Wang XQ, Wang J, Liu HM.** Simvastatin has beneficial effect on pulmonary artery hypertension by inhibiting NF-kappaB expression. *Mol Cell Biochem* 354: 77–82, 2011.
45. **Makanga M, Maruyama H, Dewachter C, Da Costa AM, Hupkens E, de Medina G, Naeije R, Dewachter L.** Prevention of pulmonary hypoplasia and pulmonary vascular remodeling by antenatal simvastatin treatment in nitrofen-induced congenital diaphragmatic hernia. *Am J Physiol Lung Cell Mol Physiol* 308: L672–L682, 2015.
46. **Mathews ES, Mawdsley DJ, Walker M, Hines JH, Pozzoli M, Appel B.** Mutation of 3-hydroxy-3-methylglutaryl CoA synthase I reveals requirements for isoprenoid and cholesterol synthesis in oligodendrocyte migration arrest, axon wrapping, and myelin gene expression. *J Neurosci* 34: 3402–3412, 2014.
47. **Mihos CG, Santana O.** Pleiotropic effects of the HMG-CoA reductase inhibitors. *Int J Gen Med* 4: 261–271, 2011.
48. **Mourani PM, Abman SH.** Pulmonary vascular disease in bronchopulmonary dysplasia: pulmonary hypertension and beyond. *Curr Opin Pediatr* 25: 329–337, 2013.
49. **Nergui S, Fukumoto Y, Do EZ, Nakajima S, Shimizu T, Ikeda S, Elias-Al-Mamun M, Shimokawa H.** Role of endothelial nitric oxide synthase and collagen metabolism in right ventricular remodeling due to pulmonary hypertension. *Circ J* 78: 1465–1474, 2014.
50. **O'Reilly M, Thébaud B.** Animal models of bronchopulmonary dysplasia. The term rat models. *Am J Physiol Lung Cell Mol Physiol* 307: L948–L958, 2014.
51. **Ose A, Kusuhara H, Endo C, Tohyama K, Miyajima M, Kitamura S, Sugiyama Y.** Functional characterization of mouse organic anion transporting peptide 1a4 in the uptake and efflux of drugs across the blood-brain barrier. *Drug Metab Dispos* 38: 168–176, 2010.
52. **Ou XM, Feng YL, Wen FQ, Huang XY, Xiao J, Wang K, Wang T.** Simvastatin attenuates bleomycin-induced pulmonary fibrosis in mice. *Chin Med J (Engl)* 121: 1821–1829, 2008.
53. **Pacary E, Tixier E, Coulet F, Roussel S, Petit E, Bernaudin M.** Crosstalk between HIF-1 and ROCK pathways in neuronal differentiation of mesenchymal stem cells, neurospheres and in PC12 neurite outgrowth. *Mol Cell Neurosci* 35: 409–423, 2007.
54. **Pedroni SM, Gonzalez JM, Wade J, Jansen MA, Serio A, Marshall I, Lennen RJ, Girardi G.** Complement inhibition and statins prevent fetal brain cortical abnormalities in a mouse model of preterm birth. *Biochim Biophys Acta* 1842: 107–115, 2014.
55. **Porter FD, Herman GE.** Malformation syndromes caused by disorders of cholesterol synthesis. *J Lipid Res* 52: 6–34, 2011.

56. **Rikitake Y, Kim HH, Huang Z, Seto M, Yano K, Asano T, Moskowitz MA, Liao JK.** Inhibition of Rho kinase (ROCK) leads to increased cerebral blood flow and stroke protection. *Stroke* 36: 2251–2257, 2005.
57. **Rysz-Górzynska M, Gluba-Brzozka A, Sahebkar A, Serban MC, Mikhailidis DP, Ursoniu S, Toth PP, Bittner V, Watts GF, Lip GY, Rysz J, Catapano AL, Banach M.** Efficacy of statin therapy in pulmonary arterial hypertension: a systematic review and meta-analysis. *Sci Rep* 6: 30060, 2016.
58. **Sartori C, Allemann Y, Trueb L, Delabays A, Nicod P, Scherrer U.** Augmented vasoreactivity in adult life associated with perinatal vascular insult. *Lancet* 353: 2205–2207, 1999.
59. **Satoh K, Fukumoto Y, Shimokawa H.** Rho-kinase: important new therapeutic target in cardiovascular diseases. *Am J Physiol Heart Circ Physiol* 301: H287–H296, 2011.
60. **Satoh M, Takahashi Y, Tabuchi T, Minami Y, Tamada M, Takahashi K, Itoh T, Morino Y, Nakamura M.** Cellular and molecular mechanisms of statins: an update on pleiotropic effects. *Clin Sci* 129: 93–105, 2015.
61. **Schachter M.** Chemical, pharmacokinetic and pharmacodynamic properties of statins: an update. *Fundam Clin Pharmacol* 19: 117–125, 2005.
62. **Schafer M, Myers C, Brown RD, Frid MG, Tan W, Hunter K, Stenmark KR.** Pulmonary arterial stiffness: toward a new paradigm in pulmonary arterial hypertension pathophysiology and assessment. *Curr Hypertens Rep* 18: 4, 2016.
63. **Schroll S, Lange TJ, Arzt M, Sebah D, Nowrotek A, Lehmann H, Wensel R, Pfeifer M, Blumberg FC.** Effects of simvastatin on pulmonary fibrosis, pulmonary hypertension and exercise capacity in bleomycin-treated rats. *Acta Physiol (Oxf)* 208: 191–201, 2013.
64. **Shi J, Wei L.** Rho kinases in cardiovascular physiology and pathophysiology: the effect of fasudil. *J Cardiovasc Pharmacol* 62: 341–354, 2013.
65. **Shimokawa H, Sunamura S, Satoh K.** RhoA/Rho-kinase in the cardiovascular system. *Circ Res* 118: 352–366, 2016.
66. **Somlyo AV.** Cyclic GMP regulation of myosin phosphatase: a new piece for the puzzle? *Circ Res* 101: 645–647, 2007.
67. **Takayasu H, Masumoto K, Hagiwara K, Sasaki T, Ono K, Jimbo T, Uesugi T, Gotoh C, Urita Y, Shinkai T, Tanaka H.** Increased pulmonary RhoA expression in the nitrofen-induced congenital diaphragmatic hernia rat model. *J Pediatr Surg* 50: 1467–1471, 2015.
68. **Thelen KM, Laaksonen R, Paiva H, Lehtimaki T, Lutjohann D.** High-dose statin treatment does not alter plasma marker for brain cholesterol metabolism in patients with moderately elevated plasma cholesterol levels. *J Clin Pharmacol* 46: 812–816, 2006.
69. **Thirunavukkarasu M, Selvaraju V, Dunna NR, Foye JL, Joshi M, Otani H, Maulik N.** Simvastatin treatment inhibits hypoxia inducible factor 1-alpha-(HIF-1alpha)-prolyl-4-hydroxylase 3 (PHD-3) and increases angiogenesis after myocardial infarction in streptozotocin-induced diabetic rat. *Int J Cardiol* 168: 2474–2480, 2013.
70. **Tijsseling D, Camm EJ, Richter HG, Herrera EA, Kane AD, Niu Y, Cross CM, de Vries WB, Derks JB, Giussani DA.** Statins prevent adverse effects of postnatal glucocorticoid therapy on the developing brain in rats. *Pediatr Res* 74: 639–645, 2013.
71. **van Loon RL, Roofthooft MT, Delhaas T, van Osch-Gevers M, ten Harkel AD, Strengers JL, Backx A, Hillege HL, Berger RM.** Outcome of pediatric patients with pulmonary arterial hypertension in the era of new medical therapies. *Am J Cardiol* 106: 117–124, 2010.
72. **Wang CY, Liu PY, Liao JK.** Pleiotropic effects of statin therapy: molecular mechanisms and clinical results. *Trends Mol Med* 14: 37–44, 2008.
73. **Woodland C, Huang TT, Gryz E, Bendayan R, Fawcett JP.** Expression, activity and regulation of CYP3A in human and rodent brain. *Drug Metab Rev* 40: 149–168, 2008.
74. **Xu EZ, Kantores C, Ivanovska J, Engelberts D, Kavanagh BP, McNamara PJ, Jankov RP.** Rescue treatment with a Rho-kinase inhibitor normalizes right ventricular function and reverses remodeling in juvenile rats with chronic pulmonary hypertension. *Am J Physiol Heart Circ Physiol* 299: H1854–H1864, 2010.
75. **Ziino AJ, Ivanovska J, Belcastro R, Kantores C, Xu EZ, Lau M, McNamara PJ, Tanswell AK, Jankov RP.** Effects of Rho-kinase inhibition on pulmonary hypertension, lung growth, and structure in neonatal rats chronically exposed to hypoxia. *Pediatr Res* 67: 177–182, 2010.